Hydrol. Earth Syst. Sci. Discuss., 12, 11331–11370, 2015
www.hydrol-earth-syst-sci-discuss.net/12/11331/2015/
doi:10.5194/hessd-12-11331-2015

Hydrology and Earth System Sciences
Open Access
Discussions

Identification of anthropogenic and natural inputs of sulfate into a karstic coastal groundwater system in northeast China: evidence from major ions, $\delta^{13}C_{DIC}$ and $\delta^{34}S_{SO_4}$

D. Han[1], **X. Song**[1], **and M. J. Currell**[2]

[1]Key Laboratory of Water Cycle & Related Land Surface Processes, Institute of Geographic Sciences and Natural Resources Research, Chinese Academy of Sciences, Beijing, 100101, China
[2]School of Civil, Environmental and Chemical Engineering, RMIT University, Melbourne, Victoria 3001, Australia

Received: 16 August 2015 – Accepted: 18 September 2015 – Published: 3 November 2015

Correspondence to: D. Han (dmeihan@gmail.com)

Published by Copernicus Publications on behalf of the European Geosciences Union.

Abstract

The hydrogeochemical processes controlling groundwater evolution in the Daweijia area of Dalian, northeast China, were characterized using hydrochemistry and isotopes of carbon and sulfur ($\delta^{13}C_{DIC}$ and $\delta^{34}S_{SO_4}$). The aim was to distinguish anthropogenic impacts as distinct from natural processes, with a particular focus on sulfate, which is found at elevated levels (range: 54.4 to 368.8 $mg L^{-1}$; mean: 174.4 $mg L^{-1}$) in fresh and brackish groundwater. The current investigation reveals minor seawater intrusion impact (not exceeding 5 % of overall solute load), in contrast with extensive impacts observed in 1982 during the height of intensive abstraction. This indicates that measures to restrict groundwater abstraction have been effective. However, hydrochemical facies analysis shows that the groundwater remains in a state of ongoing hydrochemical evolution (towards Ca-Cl type water) and quality degradation (increasing nitrate and sulphate concentrations). The wide range of NO_3 concentrations (74.7–579 $mg L^{-1}$) in the Quaternary aquifer indicates considerable input of fertilizers and/or leakage from septic systems. Both $\delta^{13}C$ (−14.5 to −5.9 ‰) and $\delta^{34}S_{SO_4}$ (+5.4–+13.1 ‰) values in groundwater show increasing trends along groundwater flow paths. While carbonate minerals may contribute to increasing $\delta^{13}C_{DIC}$ and $\delta^{34}S_{SO_4}$ values in deep karstic groundwater, high loads of agricultural fertilizers reaching the aquifer via irrigation return flow are likely the main source of the dissolved sulfate in Quaternary groundwater, as shown by distinctive isotopic ratios and a lack of evidence for other sources in the major ion chemistry. According to isotope mass balance calculations, the fertilizer contribution to overall sulfate has reached an average of 62.1 % in the Quaternary aquifer, which has a strong hydraulic connection to the underlying carbonate aquifer. The results point to an alarming level of impact from the local intensive agriculture on the groundwater system, a widespread problem throughout China.

1 Introduction

Degradation of groundwater quality, including salinization has become an increasingly serious global problem in coastal aquifers worldwide in recent years. With rapid economic development, population growth and increasing demand for fresh water resources, extensive groundwater withdrawals in these areas have led to water level declines and increasing groundwater salinization (e.g. Barlow and Reichard, 2010). Many previous studies have investigated the mechanisms of salinization and potential sources of groundwater salinity in coastal aquifers, which can include evaporite mineral dissolution (e.g. Cardenal et al., 1994), downward movement of shallow saline water into deep aquifers (e.g., Guo et al., 1995), brine intrusion (e.g., Han et al., 2011), and mixing caused by poorly constructed wells (e.g., Aunay et al., 2006), as well as "classic" seawater intrusion (e.g., Daniele et al., 2013).

Coastal areas are often sites of intensive human activity, including urbanisation and agriculture. Intensive agriculture is known to be associated in some areas with salinization (e.g. Ghassemi et al., 1995) and other groundwater quality issues such as addition of nitrate, sulphate and other compounds contained in fertilizers (e.g. Kaown et al., 2009; Currell et al., 2010). Environmental tracers, such as stable sulfur and carbon isotopes, e.g. δ^{34}S of dissolved SO_4 ($\delta^{34}S_{SO_4}$), and δ^{13}C in dissolved inorganic carbon ($\delta^{13}C_{DIC}$), and major ion chemistry have been useful in identifying sources of salinity and dissolved sulphate and carbonate species in groundwater (Sánchez-Martos et al., 2002; Schiavo et al., 2009; de Montety et al., 2008; Ghiglieri et al., 2012) and for determining water-rock interaction processes in carbonate aquifers (e.g., carbonate mineral dissolution/precipitation, cation-exchange) (Back et al., 1979; Plummer and Sprinkle, 2001; Moral et al., 2008; Daniele et al., 2013). However, to date few areas of major anthropogenic activity and known active or previous salinization from seawater intrusion have been assessed using these tracers, in order to distinguish different water quality degradation processes, such as seawater–freshwater mixing vs. input of agricultural chemicals and irrigation return flow.

Seawater intrusion was first discovered in the Dalian area in 1964 and become very serious in the early 1990s. The area is also the site of ongoing intensive agricultural activity. This study focuses on the coastal aquifers around Daweijia well field (Fig. 1), which was established in 1969 and formerly provided major water supply for Dalian City. A range of groundwater management strategies were proposed in the 1990s to reduce the threat of seawater intrusion to the aquifer (Wu, 1990; Zhao, 1991; Wu et al., 1994), culminating in the local government ceasing to supply water to Dalian City from the aquifer in 2001.

Most previous investigations in this area have focused on the mechanism of seawater intrusion and related water-rock interactions (Wu et al., 1994; Yang, 2011; Zhao et al., 2012), but have ignored the potential impact of anthropogenic contributions to groundwater salinity and water quality degradation. Little is known about the influence of agricultural practices on sulphur cycling and transport in this and other coastal aquifers impacted by intensive agriculture. Here, we report new data for C and S isotopes and major ions in groundwater from the Daweijia area, which gives new insight into sources of water quality degradation, including agriculture. Using chemical and isotopic tracers, this study identifies the different sources of sulfate, salinity and determines the major controls on hydrochemical evolution. Understanding these issues can help to prevent further deterioration of groundwater quality in this and other similar systems in north China and elsewhere around the world.

2 Study area

The investigated area (39°09′–39°13′ N and 121°37′–121°47′ E) is located in northeast China along the Bohai-Sea coast (Fig. 1). It has a catchment area of 66 km^2 to the north of Dalian City (population 3.25 million), Liaoning Province. The climate is warm temperate continental monsoon, with annual average temperature of ~ 10 °C. Most of the precipitation, totalling ~ 600 mm annually (Dalian Municipal Meteorological Bureau, 2014) falls during the June–September rainy season. The ephemeral Daweijia

River runs through the region from east to west. Under natural conditions, groundwater discharged into the sea from the southeast towards the northwest.

The geology of the Daweijia area consists of Quaternary deposits over-lying carbonate aquifers of Paleozoic (Ordovician and Cambrian) and Proterozoic (Sinian) age. Two groups of faults are developed in this area, namely NE normal faults (F1 and F2 in Fig. 1) and EW reverse faults (F3 and F4 in Fig. 1). These structural faults cut the bedrock and are the main channel for groundwater infiltration and movement, affecting the degree of subsurface karst development (Song, 2013). The main karst development sections in the Cambrian and Ordovician formation include (i) 5 to 20 m a.s.l. (near surface karst), (ii) −5 to −40 m a.s.l. (shallow karst), (iii) −50 to −85 m a.s.l. (medium depth karst), and (iv) < −90 m a.s.l. (deep karst) (Zhao, 1991). The aquifers within the Daweijia area can be divided into upper and lower aquifer systems; the upper aquifer is composed of Quaternary sediments with variable thickness of 0–40 m. This consists of gravel, sand and clay layers and is not extensively pumped for water supply. The carbonate aquifers underlying the Quaternary deposits are mainly composed of Lower Ordovician, Middle and Upper Cambrian limestone, with major karst development in the medium section between −40 and −70 m a.s.l. (Lü et al., 1981; Zhao, 1991). The most productive carbonate aquifers are distributed in the valley along Daweijia River valley. The geologic contacts and hydraulic connections between the upper and lower aquifer systems used in this study were determined from geologic logs and geophysical exploration during a previous investigation of regional hydrogeology in the Daweijia area (Lü et al., 1981; Jin and Wu, 1990).

The carbonate aquifer is pumped for agricultural and public water supply. The Daweijia well field was established in 1969 for water supply to Dalian City and at peak usage, the upper aquifer suffered extensive drawdown. Along with this, the average chloride concentration in groundwater increased from 199 mg L^{-1} in 1966 to 559 mg L^{-1} in 1991, and reached a peak of 940 mg L^{-1} in 1994. Under the restrictions on groundwater extraction enacted, the Cl value returned to 454 mg L^{-1} in 2005. This included the drastic measure of switching off the well field supplying Dalian City since 2001 (Song, 2013).

Although the groundwater levels have recovered in recent years, groundwater salinity has not completely been reversed, and elevated nitrate and sulphate concentrations have continued since this time. Potential causes include “residual” seawater intrusion which has not yet re-equilibrated with recovered water levels and/or different sources of contamination, associated with agriculture or urban activities.

Comparing background data (1962, Lü et al., 1981) and current data (2010, in this study), the average nitrate concentrations in groundwater increased from 2.1 $\mathrm{mg\,L^{-1}}$ in 1962 to 202 $\mathrm{mg\,L^{-1}}$ in 2010 in the carbonate aquifer, and mean sulfate concentration increased from 72.4 $\mathrm{mg\,L^{-1}}$ in 1962 to 150 $\mathrm{mg\,L^{-1}}$ in 2010. For the Quaternary aquifer, mean nitrate concentrations have changed from 6.7 $\mathrm{mg\,L^{-1}}$ in 1962 to 215 $\mathrm{mg\,L^{-1}}$ in 2010, and sulfate from 35.2 $\mathrm{mg\,L^{-1}}$ in 1962 to 214 $\mathrm{mg\,L^{-1}}$ in 2010.

3 Methods

3.1 Sampling and analysis

We collected 30 water samples during two sampling campaigns (June 2006 and August 2010) for analysis of major ions and stable isotopes ($\delta^{13}\mathrm{C}_{\mathrm{DIC}}$ and $\delta^{34}\mathrm{S}_{\mathrm{SO4}}$). The samples include 29 from wells and one seawater sample. Sampling wells are production wells with variable depths (8.4–128 m) and screened intervals (lengths of 2–35 m, see Table 1) and these are distributed mainly along the Daweijia River valley (Fig. 1). The screened intervals of wells in the carbonate aquifer are mainly between 65–100 m below ground surface (Table 1). Before sampling, the wells were pumped for at least for half an hour until physico-chemical parameters (e.g., water temperature, pH, electrical conductivity and dissolved oxygen) stabilised. All samples were filtered through 0.45 µm pore-size filter paper and stored in HDPE bottles at 4 °C in a cool room until analysis. The samples prepared for cation analysis were acidified to pH < 2 by adding high purity $\mathrm{HNO_3}$. Bicarbonate was determined in the field by titrating with 0.22 $\mathrm{NH_2SO_4}$. Major anions were measured by ion chromatography (SHIMADZU), and major cations were determined using ICP-AES by the Laboratory of Physics and Chemistry, Institute of Geographic Sciences and Natural Resources Research (IGSNRR), Chinese Academy of Sciences (CAS). The ion balance errors of the chemical analyses were generally within ±15 %. The hydrogeochemical code PHREEQC-2 (version 2.18.3, Parkhurst and Appelo, 1999) was used to determine the saturation indexes (SI) of calcite, dolomite and gypsum.

Analysis for ^{13}C in dissolved inorganic carbon was performed using a Finnigan MAT 252 instrument with an analytical precision of ±0.2 ‰ in the State Key Laboratory of Environmental Geochemistry, Institute of Geochemistry (Guiyang), CAS. The $\delta^{13}C_{DIC}$ values of 16 water samples are expressed in ‰ relative to Pee Dee Belemnite (V-PDB) standard. Samples for ^{34}S in dissolved sulfate in 18 groundwater samples (Table 1) were analyzed using a Finnigan MAT Delta-S gas mass spectrometer by the Laboratory for Stable Isotope Geochemistry, Institute of Geology and Geophysics, CAS. The method of Halas and Szaran (1999) was used for converting precipitated $BaSO_4$ to SO_2. The isotopic data are reported in δ (‰) notation relative to V-CDT (Canyon Diablo Trilobite). The analytical precision for water samples is better than ±0.4 ‰.

3.2 Ionic deltas and mixing calculations

To further investigate the hydrochemical behaviour of major cations and diagnose the processes modifying hydrochemical composition of groundwater in the aquifer, ionic delta values were calculated. The delta values express enrichment or depletion of particular ions relative to a conservative mixing system. These have been used in previous studies as effective indicators of groundwater undergoing freshening or salinization, along with associated water-rock interaction processes (primarily cation exchange – e.g., Appelo, 1994). It is assumed in these calculations that there is no chloride input from salts in the aquifer matrix itself, and that Cl can be regarded as the most conservative species during mixing and hydrochemical evolution. The fraction of seawater (f_{sea})

in a groundwater sample can thus be calculated using (Appelo and Postma, 2005):

$$f_{\mathrm{sw}} = \frac{C_{\mathrm{Cl,sam}} - C_{\mathrm{Cl,f}}}{C_{\mathrm{Cl,sw}} - C_{\mathrm{Cl,f}}} \tag{1}$$

where $C_{\mathrm{Cl,sam}}$, $C_{\mathrm{Cl,fresh}}$, and $C_{\mathrm{Cl,sw}}$ refer to the Cl concentration in the sample, freshwater, and seawater, respectively.

The theoretical concentration ($C_{i,\mathrm{mix}}$) of an ion i in a water sample can be calculated by comparing the measured concentration of this ion with its expected composition from conservative mixing between seawater and freshwater (Appelo and Postma, 2005):

$$C_{i,\mathrm{mix}} = f_{\mathrm{sw}} \cdot C_{i,\mathrm{sw}} + (1 - f_{\mathrm{sw}}) \cdot C_{i,\mathrm{f}} \tag{2}$$

where $C_{i,\mathrm{sam}}$ and $C_{i,\mathrm{f}}$ – the measured concentration of the ion i in the water sample and freshwater, respectively; f_{sw}-fraction of seawater. The ionic deltas (ΔC_i) of ion i can thus be obtained by:

$$\Delta C_i = C_{i,\mathrm{sam}} - C_{i,\mathrm{mix}} \tag{3}$$

4 Results

4.1 Chemical analysis

The physical and chemical characteristics of groundwater samples from the Quaternary aquifer (QA) and the Cambrian–Ordovician carbonate aquifer (COA) in the Daweijia are compiled in Table 1. Total dissolved solids (TDS) concentrations vary from 372 to 2403 $\mathrm{mg\,L^{-1}}$, with values increasing along the main direction of groundwater flow from the east towards the sea. Groundwater pH ranges from 6.5 to 7.6 with a mean of 7.2. Dissolved oxygen concentrations range from 1.3 to 8.6 $\mathrm{mg\,L^{-1}}$ with a mean of 5.6 mg L^{-1}. The fresh (< 1 g L^{-1} TDS) groundwater (e.g., CG6, CG14) is characterized as Ca-HCO_3(·Cl) type water, while brackish (1 to 10 g L^{-1} TDS) groundwater (e.g., CG7, CG10, CG11, CG17) is predominantly Ca-Cl type in the carbonate aquifer. Brackish groundwater in the shallow Quaternary aquifer was observed to be Ca-Cl·SO_4 type water, or near the coastline, (e.g., QG10, QG11) Na·Ca-Cl(·HCO_3) type. The calculated seawater fractions in groundwater based on the Cl mass balance were all less than or equal to 4.8 %. The groundwater in this study is characterized by a wide range of sulfate concentrations between 54.4 and 368.8 mg L^{-1}, with a mean value of 174.4 mg L^{-1}. Nitrate concentrations ranged from 43.1 to 579.4 mg L^{-1} with a mean value of 206.9 mg L^{-1}, far beyond the drinking water standard (50 mg L^{-1}) in China. The investigated seawater sample also has a very high nitrate concentration of 1092 mg L^{-1}. The wide range of NO_3 concentrations, indicate considerable anthropogenic input under human activities (e.g., fertilizer usage during irrigation, leakage from septic system), which is responsible for the deterioration of local groundwater and near shore sea-water quality.

The ionic delta values are plotted in Fig. 2, illustrating the varied distribution of geochemical types and evolution in the aquifer. Generally most groundwater samples are characterized by negative ΔNa^+ values and positive ΔCa^{2+} values. Some brackish groundwater samples have negative ΔNa^+ values and positive $\Delta Ca^{2+} + \Delta Mg^{2+}$ values, displaying a deficit of Na^+ with a corresponding excess in Ca^{2+} and Mg^{2+}. There are positive values of ΔSO_4^{2-} observed in most groundwater sample, and these are particularly high in the brackish groundwater (Fig. 2d).

4.2 Dissolved inorganic carbon (DIC) and $\delta^{13}C_{DIC}$

Figure 3 presents the $\delta^{13}C_{DIC}$ isotope data and this can be used to infer the sources and evolution of dissolved inorganic carbon in the investigated groundwater (Clark and Fritz, 1997). The measured $\delta^{13}C_{DIC}$ values in groundwater range from −14.5 to −5.9 ‰ vs. PDB, with a mean value of −10.5 ‰ (Table 1). The water samples from the carbonate aquifer show a relatively narrow range of $\delta^{13}C_{DIC}$ values (−12 to −8.4 ‰ with a mean value of −10.1 ‰, $n = 8$) comparable to the range of $\delta^{13}C_{DIC}$ values (−14.5 to −5.9 ‰, mean of −10.0 ‰, $n = 7$) from the Quaternary aquifer. The waters collected in the upstream areas show $\delta^{13}C$ values from −14.5 to −12.8 ‰, while the middle area has values of −12.0 to −9.0 ‰ and the coastline values between −10.6 to −5.9 ‰ (Fig. 3, Table 1).

The local seawater sample (SW1) has a $\delta^{13}C_{DIC}$ value of −3.3 ‰, which is relatively low compared to other reported values of modern seawater (−1–+2 ‰, Clark and Fritz, 1997). Carbon in C_4 plants, which include maize, sugar cane and sorghum, has $\delta^{13}C$ values that range from −10 to −16 ‰ with a mean value of ~ −12.5 ‰, while most C_3 plants have $\delta^{13}C$ values that range from −24 to −30 ‰ with an average of ~ −27 ‰ (Vogel, 1993). The evolution of DIC and $\delta^{13}C_{DIC}$ in the carbonate system begins with atmospheric CO_2 with $\delta^{13}C$ value ~ −7 ‰ VPDB, while subsequent dissolution of soil gas carbon dioxide leads to depletion of the carbon depending which source of vegetation is dominant (Clark and Fritz, 1997). Maize is the main agricultural product in the study area (Hu, 2010), indicating a C_4 vegetation source may be dominant, leading to values in the range observed (e.g. −5.9 to −14.5 ‰). Carbonate dissolution and/or exchange leads to progressive enrichment of $\delta^{13}C$ values towards the values of the mineral, usually with values between −2 and +2 ‰.

4.3 Stable isotopes of sulfate

The $\delta^{34}S_{SO_4}$ compositions varied between +5.4 and +13.1 ‰ (Table 1). Sample CG1, with a sampling depth of 100 m and collected from the centre of a residential area, has the highest $\delta^{34}S_{SO_4}$ value (+13.1 ‰). The lowest $\delta^{34}S_{SO_4}$ value (+5.4 ‰) was found for sample QG3 collected in an upstream area. Water samples from the carbonate aquifer are denoted with dashed line in Fig. 4 and have relatively high $\delta^{34}S_{SO_4}$ values (ranging from +6.6 to +13.1 ‰ with mean value of +9.9 ‰, $n = 9$) and low SO_4/Cl ratios. The groundwater samples from the Quaternary aquifer are characterized by a relatively narrow range of $\delta^{34}S_{SO_4}$ values (ranging from +5.4 to +10.1 ‰ with mean value of +7.9 ‰, $n = 8$) and wider range of SO_4/Cl ratios. Some brackish groundwater (QG2 and QG10) from the Quaternary aquifer also shows these characteristics (Fig. 4). In general, the $\delta^{34}S_{SO_4}$ values increase with correspondingly lower SO_4/Cl ratios in the direction of the coastline.

5 Discussion

A number of key geochemical processes control the evolution of groundwater in the study area. Some of these processes show evidence of taking place in both carbonate and Quaternary aquifers, while others are more confined to one of the aquifers. The major hydrochemical processes occurring in each aquifer are summarized in Table 2, which also includes a description of lines of evidence used to infer the process (in most cases 2 supporting lines of evidence exist) and links to the relevant figure.

5.1 Seawater intrusion, freshening and cation exchange

According to mixing calculations, minor seawater intrusion near the coastline is identified (Fig. 2), however the fraction of seawater does not exceed 5 % and this compares with a fraction of 20.8 % observed in 1982 (Wu et al., 1994). Hence, widespread seawater intrusion appears to be a thing of the past, although local salinization continues around the well field.

Stuyfzand (1986, 2008) proposed base-exchange indices ($BEX_D = Na + K - 0.8768 \times Cl$) for indicating intrusion or freshening of coastal aquifers based on the sequence of cation exchange reactions taking place during these processes. Apart from QG11, with positive BEX_D values, most groundwater samples are characterized by negative BEX_D values, indicating that if base-exchange is the process changing ionic ratios, then the system is actually salinizing. This is inconsistent with the trend in Cl values since

Title Page
Abstract Introduction
Conclusions References
Tables Figures
◀| |▶
◀ ▶
Back Close
Full Screen / Esc
Printer-friendly Version
Interactive Discussion

groundwater abstraction was limited, and so alternative processes must be invoked to explain the major cation compositions observed.

A similar conclusion can be drawn using the multi-rectangular HFE-diagram (Fig. 5). This classification method proposed by Giménez-Forcada (2010) can be employed to determine the dynamics of seawater intrusion, considering the percentages of major ions, showing the intruding and freshening phases in hydrochemical facies evolution. The fresh water in the recharge area mainly belongs to the Ca-MixHCO_3 (14) facies, and seawater belongs to the Na-Cl (4) facies. Most of the groundwater samples don't follow the predicted succession of facies along the mixing line (4-7-10-13), and rather indicate a small degree of simple mixing between fresh and seawater components, along with inverse cationic exchange between Na and Ca. This leads to the water reaching the Ca-Cl (16) facies observed in brackish groundwater in the carbonate aquifer. The surplus Ca^{2+} from ion exchange may also cause super-saturation with respect to calcite and dolomite; consistent with the observed positive values in the majority of samples (Langmuir, 1971). Net dissolution of carbonate minerals is not evident as a major process in the groundwater, as is shown by a number of lines of evidence below (Mg/Ca ratios, stable istopes of DIC – see Table 2). Cation exchange is thus considered crucial to the development of the Ca-Cl facies in the more evolved waters.

Generally most groundwater samples collected from the west of Daweijia well field are characterized by depletion of Na^+ more or less balanced by equivalent enrichment of Mg^{2+} plus Ca^{2+}. Both ΔNa^+ and ΔMg^{2+} decrease with an increasing fraction of seawater (f_{sw}), especially for $f_{sw} > 3\%$ (Fig. 2), which would be more characteristic of a salinization-driven base exchange process (Appelo and Postma, 2005). This may suggest a residual effect from the previous saline intrusion which is yet to re-equilibrate with the aquifer matrix. Most groundwater samples from the carbonate aquifer show ΔCa^{2+}, ΔMg^{2+}, and ΔSO_4^{2-} increases with salinity whereas ΔNa^+ decreases as salinity increases (Fig. 2), consistent with inverse cation exchange.

For fresh groundwater in the carbonate aquifer, the ionic deltas values are close to 0, indicating the modifying processes are controlled by conservative mixing and there has been little chemical interaction between the groundwater and the aquifer material. Compared to the conservative mixing, the excess of SO_4 observed (positive ΔSO_4^{2-} values) might be attributed to gypsum dissolution, under the influence of seawater intrusion (creating temporary under-saturation). However, only greater degrees of seawater intrusion can cause gypsum dissolution to result in the SO_4 excess (Daniele et al., 2013), and the chloride data are inconsistent with ongoing seawater intrusion. It can therefore be inferred that there must be an additional source of SO_4. Anthropogenic fertilizer input may explain the increases in SO_4^{2-} NO_3^- and possibly even Ca^{2+} and Cl^- in the aquifer, as is discussed further below.

5.2 Groundwater interaction with carbonate minerals

The dissolution of calcite and dolomite can be expressed by followed reactions:

$$CaCO_{3[calcite]} + CO_2 + H_2O \leftrightarrow Ca^{2+} + 2HCO_3^- \tag{R1}$$

$$CaMg(CO_3)_{2[dolomite]} + 2CO_2 + 2H_2O \leftrightarrow Ca^{2+} + Mg^{2+} + 4HCO_3^- \tag{R2}$$

$$CaCO_{3[calcite]} + CaMg(CO_3)_{2[dolomite]} + 3CO_2 + 3H_2O \leftrightarrow 2Ca^{2+} + Mg^{2+} + 6HCO_3^- \tag{R3}$$

Reaction (R3) is derived from Reactions (R1) and (R2) and expressed for concurrent dissolution of two minerals. Wang et al. (2006) calculated two “types” of calcium, namely non-gypsum and non-carbonate source calcium, for evaluating the effect of the dissolution of the major minerals (i.e., calcite, dolomite, and gypsum) in a carbonate aquifer. If we were to assume all SO_4^{2-} is from gypsum dissolution, non-gypsum source calcium can be calculated by $[Ca^{2+}]$-$[SO_4^{2-}]$ (in $mmol\,L^{-1}$). Based on the stoichiometry of Reaction (R3), non-carbonate source calcium can be expressed as $[Ca^{2+}]$-$0.33[HCO_3^-]$ (in $mmol\ L^{-1}$). Figure 6a and b shows the relations between the “non-gypsum” sourced Ca^{2+} and HCO_3^-, and between Mg^{2+} and HCO_3^-, respectively. The ratios of Ca^{2+} : HCO_3^- (in $mmol\,L^{-1}$) of most groundwater samples, especially from the carbonate aquifer, fall above the 1 : 2 and the 1 : 4 lines in Fig. 6a and shift from the

1 : 4 line in Fig. 6b. These indicate water chemistries could to some extent originate from calcite and dolomite net dissolution in accordance with the reactions above. Some of the water samples from the Quaternary aquifer are scattered around the 1 : 1 line (Fig. 6c), suggesting congruent gypsum dissolution, consistent with saturation index values of less than −0.5 for gypsum in these samples.

Concentrations of DIC in fresh and brackish groundwater were in the range of 60.1–446.5 mg L^{-1} (average 189.2 mg L^{-1}) and 46.2–512.7 mg L^{-1} (average 203.1 mg L^{-1}), respectively (Table 1). The $\delta^{13}C_{DIC}$ values of groundwater ranging from −14.5 to −5.9 ‰ vs. PDB are similar to groundwater from carbonate aquifers in southwest China, which has typical values, ranging from −15.0 to −8.0 ‰ (Li et al., 2010). The $\delta^{13}C_{DIC}$ in groundwater shows a negative correlation with DIC concentration, particularly in the karst aquifer (Fig. 3). This indicates that simple, congruent dissolution of carbonate minerals is not a major source of DIC in the groundwater. Rather, $\delta^{13}C_{DIC}$ may undergo progressive equilibration with aquifer carbonate during sequential carbonate dissolution/precipitation reactions (e.g. de-dolomitization). This is consistent with the increasing Mg/Ca ratios observed along the flow path, along with increasing $\delta^{13}C_{DIC}$ values in the carbonate aquifer (see Fig. 7a), but no overall increase in HCO_3 (Fig. 3 and Table 2). Near the coastline, the more enriched $\delta^{13}C_{DIC}$ values and lower DIC may also result due to mixing with seawater. An increasing trend in SO_4 and Mg concentrations and Mg/Ca ratios along the flow path are also indicative of de-dolomitization (e.g. Jones et al., 1989; Plummer et al., 1990; López-Chicano et al., 2001; Szynkiewicz et al., 2012) in which the dissolution of gypsum and anhydrite lead to over-saturation and thus dolomite dissolution and calcite precipitation. For deeper carbonate groundwater underlying the Daweijia wellfield, the negative correlation between Ca^{2+} and $\delta^{13}C_{DIC}$ (Fig. 7b) also indicate Ca enrichment in groundwater may be not attributed to carbonate dissolution. The increase in $\delta^{13}C$ with decreasing Ca content is likely related to the incongruent reaction, which removes Ca from solution and progressively increases $\delta^{13}C$ to equilibrate with the aquifer matrix. In the Quaternary aquifer, the minor calcite dissolution occurring could lead to increasing $\delta^{13}C$ with increasing Ca. Perhaps an alternative process may remove the HCO_3 (e.g. CO_2 de-gassing).

Dolomite dissolution is likely to add Ca^{2+}, Mg^{2+}, and HCO_3^- to the solution, while calcite precipitation will remove DIC and retain calcite saturation, resulting in generally increasing Mg/Ca ratios along flow paths, along with increasing $\delta^{13}C$ values (Freeze and Cherry, 1979; Edmunds et al., 1987; Cardenal et al., 1994; Kloppmann et al., 1998). The dissolution of even very small amounts of gypsum may cause this process to occur in carbonate aquifers, which usually characterized by near saturation with respect to calcite, by creating temporary under-saturation (due to the addition of calcium but not bicarbonate ion) (Plummer et al., 1990; López-Chicano et al., 2001; Moral et al., 2008; Szynkiewicz et al., 2012).

In pure water, a Ca/SO_4 ratio equal to 1 ($CaSO_4{\cdot}2H_2O_{[gypsum]} \leftrightarrow Ca^{2+} + SO_4^{2-} + 2H_2O$) would distinguish gypsum dissolution from other sources of sulfate salinity such as seawater (0.36) (Clark and Fritz, 1997). The Ca/SO_4 ratios of the groundwater samples range from 1.3 to 6.9, while the majority of groundwater is saturated with respect to calcite and dolomite, suggesting an additional source of Ca. This is again consistent with reverse cation exchange.

Another possible control on the carbon chemistry of the groundwater is that active re-circulation of water is taking place in the unsaturated zone of the aquifer due to anthropogenic activity. In the local agricultural soils, CO_2 concentration is usually high, with a $\delta^{13}C_{DIC}$ between −6.3 and −13.1 ‰ and $\delta^{13}C$ of dissolved organic carbon between −23.2 and −21.8 ‰ (Yang, 2011). During recharge events, water dissolves the soil CO_2 which is involved in carbonate dissolution and becomes part of the DIC pool. If this process is conducted over successive irrigation, the HCO_3^- concentration increases and $\delta^{13}C_{DIC}$ will deplete owing to the dissolved biogenic CO_2 in soil.

5.3 Sources of dissolved SO_4 to groundwater

Dissolved SO_4^{2-} of groundwater in the coastal aquifers might originate from several sources, potentially including (i) natural and artificial sulfates in rainwater; (ii) dissolution of sulphate-bearing evaporates (e.g. gypsum and anhydrite), (iii) seawater, (iv) anthropogenic pollutants (e.g. domestic sewage, detergent and agricultural fertilizers). The $\delta^{34}S$ of groundwater SO_4 are used as a tracer to identify the sources of dissolved SO_4^{2-} to the groundwater in this study. Figure 4 shows the relation between $\delta^{34}S_{SO_4}$ values and SO_4/Cl for groundwater samples, showing typical literature values for sulfur isotopic composition of major sulphate sources. Most of water samples from the Daweijia area have sulfur isotopic compositions that reflect mixed sources. The $\delta^{34}S_{SO_4}$ values are generally lower in the upstream area (+5.4 to +5.7 ‰) increasing along the groundwater flow paths towards the coast (+13.1 ‰). Enrichment in $\delta^{34}S_{SO_4}$ may result from sulphate reduction, whereas sulphide oxidation generally leads to negative $\delta^{34}S_{SO_4}$ values (Clark and Fritz, 1997). However, there are no negative $\delta^{34}S_{SO_4}$ values observed in this study area, indicating minor or negligible sulphide (such as pyrite) oxidation occurring in the aquifer.

$\delta^{34}S_{SO_4}$ value of modern seawater is approximately +21 ‰ (Rees et al., 1978). The $\delta^{34}S_{SO_4}$ of groundwaters, ranging from +13.1 to +5.4 ‰ with a mean value of +8.9 ‰, thus generally discount this as a significant source of sulphate, consistent with the low mixing fractions calculated using Cl. The $\delta^{34}S_{SO_4}$ values of precipitation from 8 stations in the north region of Yangtze River ranges from +4.9 % to +11.0 ‰ (Hong et al., 1994). Aside from CG1, the $\delta^{34}S_{SO_4}$ compositions of the samples overlap with the isotopic range of rainfall. However, rainfall is characterized by higher SO_4/Cl (2.26, Zhang et al., 2012) than the groundwater (0.16–0.97) and significantly lower total concentrations than are observed; indicating that this is only a partial origin of sulfate in groundwater. Sulfate minerals (gypsum, anhydrite, etc.) from marine sources typically have $\delta^{34}S_{SO_4}$ values between +9 and +30.2 ‰ (Shi et al., 2004; Vitòria et al., 2004). As groundwater flows downwards into the deeper karst aquifer, the $\delta^{34}S$ values increase and approach the values in marine evaporites, part of the continuous de-dolomitization reaction discussed above. However, this can not explain the observed sulfate levels in the Quaternary aquifer (see mass balance calculations below).

Fertilizers have a wide range of $\delta^{34}S_{SO_4}$ values ranging from −6.5 to +11.7 ‰, with a mean value of +3.7 ‰ and −0.8 ‰ in the Northern Hemisphere (Szynkiewicz et al., 2011) and China (Li et al., 2006), respectively. Apart from CG1 ($\delta^{34}S_{SO_4}$ value of +13.1 ‰), the $\delta^{34}S_{SO_4}$ values of the rest groundwater samples are within the $\delta^{34}S_{SO_4}$ ranges of known fertilizers. The isotopic $\delta^{34}S$ values in fertilizers significantly differ from the geological SO_4 inputs of sedimentary origin, and over-lap with most of the observed compositions (Fig. 4). In addition the very high nitrate concentrations observed in the groundwater (up to 625 mg L^{-1}) strongly indicate a high input of excess fertilizer residue via irrigation returns to the aquifer. This indicates that sulfate in fertilizers should be taken into account as a major contributing source of dissolved SO_4 in groundwater, especially from the Quaternary aquifer. This is also confirmed by the general positive relationship between NO_3^- and SO_4^{2-} concentrations (Fig. 8a) and correlation (albeit weak) between $\delta^{34}S$ values and NO_3 concentrations in the Quaternary aquifer (Fig. 8b). It can be assumed that other anthropogenic sources of SO_4 such as atmospheric deposition or detergents from domestic/wastewater sources, or pig manure are negligible in the study area.

Despite they clear overlap in $\delta^{34}S$ of fertilizers and groundwater SO_4^{2-}, the $\delta^{34}S$ measured in upstream locations (e.g. QG3 and QG4) probably reflect inputs from geologic SO_4 sources (such as soil sulfate) (Fig. 4). In contrast, the sulfur isotope values are more consistent with marine sedimentary sources of groundwater SO_4 in the carbonate aquifer, due to the sustained water-rock interaction and longer residence time. The evidence for gypsum dissolution as part of de-dolomotization in the major ion and carbon isotope data (discussed above) is also consistent with a marine evaporite source of sulphur in the deeper aquifer.

Both δ^{13}C and $\delta^{34}S_{SO_4}$ values increase along the groundwater flow path. Groundwater with low δ^{13}C values (e.g. −14.5 ‰) and $\delta^{34}S_{SO_4}$ values (e.g. ~ +5.4 ‰) represents recently recharged water, which is dominated by unsaturated zone processes and diffuse flow. Equilibration with carbonate minerals in the aquifer matrix during dedolomitization makes an important contribution to the groundwater δ^{13}C evolution in the karst aquifer (δ^{13}C up to −5.9 ‰ in QG11), reaching saturation with respect to calcite and dolomite. Then, the high loads of fertilizers accessible during agricultural return flow are the most likely source of the dissolved sulfate and nitrate, particularly in the shallow Quaternary aquifer.

5.4 Anthropogenic contribution on groundwater chemistry and environmental implications

Fertilizers are applied beyond what is taken up by crops in the long term in many parts of China (Davidson and Wei, 2012) as evident from the high NO_3^- concentrations in groundwater. NO_3^- concentrations are obviously elevated (e.g. 75–386 mg L^{-1}) in the shallow groundwater from the Quaternary aquifer, especially near the Daweijia well field, resulting from agricultural fertilization. Due to nitrate input from fertilizers, the relatively low nitrate concentrations in some deep groundwater (e.g. CG4, CG14), which are located in the upstream area, show that, compared with groundwater in the downgradient area, these waters have locally reduced impacts from contamination. However, many deep groundwater samples have similar ranges of NO_3^- concentrations to shallow groundwaters, indicating that there is hydraulic connection between shallow and deep aquifers (e.g. QG5 and CG7 in Fig. 9).

To quantify the fertilizers contributions to groundwater chemistry, we considered the inputs of precipitation infiltration, seawater intrusion and evaporite dissolution into groundwater system. We used a mass balance approach to evaluate the contribution of difference sources of sulphate to the dissolved SO_4^{2-} of groundwater. The four sources of sulphate in the dissolved SO_4^{2-} of groundwater are from precipitation, seawater, fertilizer and evaporate dissolution. The isotopic composition of groundwater sulphate ($\delta^{34}S_{SO_4}$) can be calculated by:

$$\begin{aligned}\delta^{34}S_{gw} \times SO_{4,gw} = {} & \delta^{34}S_{prec} \times SO_{4,prec} + \delta^{34}S_{sw} \times SO_{4,sw} \\ & + \delta^{34}S_{fer} \times SO_{4,fer} + \delta^{34}S_{evp} \times SO_{4,evp}\end{aligned} \tag{R4}$$

where $\delta^{34}S_{prec}$, $SO_{4,prec}$, $\delta^{34}S_{sw}$, $SO_{4,sw}$, $\delta^{34}S_{fer}$, $SO_{4,fer}$, $\delta^{34}S_{evp}$, and $SO_{4,evp}$, correspond to the end member $\delta^{34}S$ values for rainfall (+5.39 ‰, Hong et al., 1994), seawater (+21 ‰, Clark and Fritz, 1997), fertilizer (–0.8 ‰, Li et al., 2006), and sulfate marine evaporates of Cambrian–Ordovician age (+28 ‰, Clark and Fritz, 1997). The dissolved SO_4^{2-} concentration ($SO_{4,gw}$) in groundwater is the total sulphate contribution from precipitation, seawater, fertilizer and evaporate:

$$SO_{4,gw} = SO_{4,prec} + SO_{4,sw} + SO_{4,fer} + SO_{4,evp} \tag{R5}$$

where

$$SO_{4,prec} = \left[SO_{4,prec}\right] \times R = 8.02\,\mathrm{mg\,L^{-1}} \times 0.783 \tag{R6}$$

$$SO_{4,sw} = \left[SO_{4,sw}\right] \times f_{sw} = 2710\,\mathrm{mg\,L^{-1}} \times f_{sw} \tag{R7}$$

The SO_4^{2-} concentration ($[SO_{4,prec}] = 8.02\,\mathrm{mg\,L^{-1}}$) of the local precipitation was reported by Zhang et al., 2012, and SO_4^{2-} concentration ($[SO_{4,sw}] = 2710\,\mathrm{mg\,L^{-1}}$) of the seawater referenced from Clark and Fritz, 1997. R is the recharge rate equal to the ratio of the amount of precipitation infiltration and the amount of the total groundwater resources in the study area. According to the water balance calculations in the local groundwater flow system (CGS, 2007), groundwater is mainly recharged from precipitation infiltration, which occupied 78.3 % (R) of the total recharge water volume. f_{sw} can be calculated by the Eq. (1) for each groundwater sample.

Title Page
Abstract Introduction
Conclusions References
Tables Figures
◂◂ ▸▸
◂ ▸
Back Close
Full Screen / Esc
Printer-friendly Version
Interactive Discussion

The results of the mass balance, showing sulphate contribution to groundwater from fertilizer (assuming these end-members correspond to values in the study area) are shown in Fig. 10. In total, 4 to 22 % of the dissolved SO_4^{2-} concentrations in groundwater are contributed from evaporite dissolution, whereas 30 to 75 % of the dissolved SO_4^{2-} concentrations in groundwater can be ascribed to input from fertilizers. According to these calculations, overall, the local application of the fertilizers is now responsible for the majority of dissolved SO_4^{2-} in groundwater. The contribution reaches on average 62.1 % in the Quaternary aquifer and 48.7 % in the deeper carbonate aquifer; showing that the shallow Quaternary aquifer is particularly prone to pollution by fertilizer utilization. The sulphate contributions to groundwater from seawater and precipitation are less than 10 %, which is relatively lower and is consistent with the observation that pumping restrictions have effectively halted saline intrusion in the area. Although further investigation is needed to determine the contribution of dissolved sulphate from different pollution sources (the end-member values used above are naturally uncertain and may bias the overall % contributions), the current results indicate that the anthropogenic contaminant input plays dominant role in providing sulfate to the shallow groundwater (as well as nitrate), and that this influence has extended into the deeper carbonate aquifer. This widespread shift towards agricultural return flow becoming the dominant control on groundwater chemistry, particularly in shallow aquifers, is consistent with what is unfolding over many areas of northern China (Currell et al., 2012). This is a disturbing trend, particularly given the time-lags involved in groundwater systems equilibrating towards new water quality norms, which suggest significant future degradation of groundwater resources will continue to occur in these areas.

6 Conclusions

The coastal aquifer in the Daweijia area, northeast China is composed of interlayered Quaternary sedimentary and Cambrian–Ordovician carbonate rocks. The groundwater has evolved from fresh water (meteoric recharge) to brackish water in series of water types: Ca(·Mg)-HCO_3·Cl → Ca·Na-Cl·HCO_3 → Ca-Cl → Na·Ca-Cl → Na-Cl via a combination of natural and anthropogenic processes, mainly equilibration with carbonate minerals in the aquifer matrix (de-dolomitization, involving gypsum dissolution), cation exchange and fertilizer input. This indicates that the local government efforts to restrict groundwater abstraction have been effective in their purpose of limiting saline intrusion. However, water quality degradation still is occurring, mostly in the form of nitrate and sulphate contamination.

There are the increasing trends of $\delta^{13}C_{DIC}$ and $\delta^{34}S_{SO_4}$ values for groundwater along the flow path. The high hydrochemical ion ratios (non-gypsum source Ca/HCO_3 and Mg/HCO_3) show that congruent dissolution carbonate minerals make limited contributions to the increasing $\delta^{13}C_{DIC}$ and $\delta^{34}S_{SO_4}$ values in groundwater. The potential sources of dissolved SO_4^{2-} in the coastal aquifers include natural and artificial sulfates in rainwater, dissolution of sulfate evaporates (e.g. gypsum and anhydrite), seawater, and anthropogenic pollutants (e.g. agricultural fertilizers). We estimated the contributions of the four different sources on the dissolved sulphate in groundwater quality by using mass balance approach. Apart from seawater and precipitation (less than 10 %), the fertilizer contribution in sulphate concentrations of groundwater could be as high as an average of 62.1 % in the Quaternary aquifer, and 48.7 % in the deeper carbonate aquifer, depending on the end-member composition used. Although the processes that affect the groundwater quality and the contribution to the dissolved sulfate of groundwater in the Daweijia area should be further evaluated by more investigation (such as nitrogen isotope data), the current research results obtained from a set of geochemical and isotopic tools show the sulfate contribution from fertilizer application, compared with that from seawater intrusion and precipitation infiltration, is dominant, with a secondary source from long-term evaporite dissolution and de-dolomitization as water equilibrates with the carbonate aquifer matrix.

Also, there are similar ranges of NO_3^- concentrations, isotopic compositions ($\delta^{13}C_{DIC}$ and $\delta^{34}S_{SO_4}$) and water type in the shallow Quaternary and deeper carbonate aquifers in most parts of the study area, indicating interaction between shallow and deep groundwater in the study area, which has implications for aquifer protection from contamination by agricultural chemicals.

Acknowledgements. This research was partially funded by the strategic science and technology project of the Exploring Advanced Discipline (no. 2012QY007) in the Institute of Geographic Sciences and Natural Resources Research, Chinese Academy of Sciences. It was undertaken as part of a groundwater survey project entitled "Assessment of Vulnerability and Investigation of Environmental Geology in the Key Section of Circum-Bohai-Sea Region". The authors are grateful to Yang Jilong, Liu Xin, Xie Hailan and Pan Tong for their help and support during water sampling and monitoring in the field and data collection. We also want to acknowledge the support from Tianjin Institute of Geology and Mineral Resources and Liaoning Hydrological and Engineering Geological Prospecting Academy in Dalian.

References

Appelo, C. A. J.: Cation and proton exchange, pH variations and carbonate recactions in a freshening aquifer, Water Resour. Res., 30, 2793–2805, 1994.

Appelo, C. A. J. and Postma, D.: Geochemistry, Groundwater and Pollution, 2nd Edn., A. A. Balkema Publishers, Leiden, the Netherlands, 2005.

Aunay, B., Dörfliger N., Duvail, C., Grelot, F., Le Strat, P., Montginoul, M., and Rinaudo, J. D.: Hydro-socio-economic implications for water management strategies: the case of Roussillon coastal aquifer, in: International Symposium – DARCY 2006, Aquifer Systems Management, May 2006, Dijon, France, p. 9, 2006

Back, W., Hanshaw, B. B., Pyle, T. E., Plummer, L. N., and Weidie, A. E.: Geochemical Significance of Groundwater Discharge and Carbonate Solution of the Formation of Caleta Xel Ha, Quintana Roo, Mexico, Water Resour. Res., 15, 1521–1535, 1979.

Barlow, P. M. and Reichard, E. G.: Saltwater intrusion in coastal regions of North America, Hydrogeol. J., 18, 247–260, 2010.

Cardenal, J., Benavente, J., and Cruz-Sanjulián J. J.: Chemical evolution of groundwater in Triassic gypsum-bearing carbonate aquifers (Las Alpujarras, southern Spain), J. Hydrol., 161, 3–30, 1994.

CGS (China Geology Survey): Assurance report of water supply in Dalian City, Geological survey institute of Liaoning Province, Dalian, China, 38–44, 2007.

Clark, I. and Fritz, P.: Environmental Isotopes in Hydrogeology, Lewis Publishers, Boca Raton, 1997.

Cravotta, C. A.: Use of Stable Isotopes of Carbon, Nitrogen, and Sulfur to Identify Sources of Nitrogen in Surface Waters in the Lower Susquehanna River Basin, Pennsylvania, US Geol. Surv. Water, Supply Paper, Denver, 2497, 1997.

Currell, M. J., Cartwright, I., Bradley, D. C., and Han, D. M.: Recharge history and controls on groundwater quality in the Yuncheng Basin, north China, J. Hydrol., 385, 216–229, 2010.

Currell, M. J., Han, D. M., Chen, Z. Y., and Cartwright, I.: Sustainability of groundwater usage in northern China: dependence on palaeowaters and effects on water quality, quantity and ecosystem health, Hydrol. Process., 26, 4050–4066, 2012.

Daniele, L., Vallejos Á., Corbella, M., Luis Molina, L., and Pulido-Bosch, A.: Hydrogeochemistry and geochemical simulations to assess water-rock interactions in complex carbonate aquifers: the case of Aguadulce (SE Spain), Appl. Geochem., 29, 43–54, 2013.

de Montety, V., Radakovitch, O., Vallet-Coulomb, C., Blavoux, B., Hermitte, D., and Valles, V.: Origin of groundwater salinity and hydrogeochemical processes in a confined coastal aquifer: case of the Rhône delta (Southern France), Appl. Geochem., 23, 2337–2349, 2008.

Edmunds, W. M., Cook, J. M., Darling, W. G., Kinniburgh, D. G., and Miles, D. L.: Baseline geochemical conditions in the chalk aquifer, Berkshire, UK: a basis for groundwater quality management, Appl. Geochem., 2, 251–274, 1987.

Fan, J. J.: Seawater intrusion and calculation of groundwater exploitation in the karst area of the west JinXian, Dalian, Hydrogeology and Eng. Geol., 1, 3–6, 1984 (in Chinese with English abstract).

Freeze, R. A. and Cherry, J. A.: Groundwater, Prentice Hall, Englewood Cliffs, NJ, 604 pp., 1979.

Ghassemi, F., Jakeman A. J., and Nix H. A.: Salinisation of Land and Water Resources: Human Causes, Extent, Management and Case Studies, University of New South Wales Press, Sydney, 526 pp., 1995.

Ghiglieri, G., Carletti, A., and Pittalis, D.: Analysis of salinization processes in the coastal carbonate aquifer of Porto Torres (NW Sardinia, Italy), J. Hydrol., 432–433, 43–51, 2012.

Giménez-Forcada, E.: Dynamic of sea water interface using hydrochemical facies evolution diagram, Ground Water, 48, 212–216, 2010.

Grassi, S. and Cortecci, G.: Hydrogeology and geochemistry of the multilayered confined aquifer of the Pisa plain (Tuscany-Central Italy), Appl. Geochem., 20, 41–54, 2005.

Guo, Y. H., Shen, Z. L., and Zhong, Z. X.: Downward movement of shallow saline groundwater and its impact on deep-lying groundwater system, Hydrogeology and Eng. Geol., 2, 8–12, 1995 (in Chinese with English abstract).

Halas, S. and Szaran, J.: Low-temperature thermal decomposition of sulfates to SO_2 for on-line $^{34}S/^{32}S$ analysis, Anal. Chem., 71, 3254–3257, 1999.

Han, D. M., Kohfahl, C., Song, X. F., Xiao, G. Q., and Yang, J. L.: Geochemical and isotopic evidence for palaeo-seawater intrusion into the south coast aquifer of Laizhou Bay, China, Appl. Geochem., 26, 863–883, 2011.

Hong, Y. T., Zhang, H. B., Zhu, Y. X., Pu, H. C., Jiang, H. B., and Liu, D. P.: Characteristics of sulfur isotope composition of precipitation in China, Advances in Natural Sciences, 6, 741–745, 1994 (in Chinese).

Hosono, T., Nakano, T., Iget, A., Tayasu, I., Tanaka, T., and Yachi, S.: Impact of fertilizer on a small watershed of Lake Biwa: use of sulfur and strontium isotopes in environmental diagnosis, Sci. Total Environ., 384, 342–354, 2007.

Hu, T.: Analysis on economic benefit of Dalian suburban farming, Chinese Agricultural Science Bulletin, 26, 393–397, 2010 (in Chinese with English abstract).

Jin, Y. J. and Wu, Q.: The application of the electrical logging of well fluid in determining the vertical heterogeneity of sea water intrusion, Journal of Heibei College of Geology, 13, 69–73, 1990 (in Chinese with English abstract).

Jones, B., Pleydell, S. M., Ng, K.-C., and Longstaffe, F. J.: Formation of poikilotopic calcite–dolomite fabrics in the Oligocene–Miocene Bluff formation of Grand Cayman, British West Indies, B. Can. Petrol. Geol., 37, 255–265, 1989.

Kaown, D., Koh, D.-C., Mayer, B., and Lee, K.-K.: Identification of nitrate and sulphate sources in groundwater using dual stable isotope approaches for an agricultural area with different land use (Chuncheon, mid-eastern Korea), Agr. Ecosyst. Environ., 132, 223–231, 2009.

Kloppmann, W., Dever, L., and Edmunds, W. M.: Residence time of chalk groundwaters in the Paris Basin and the North German Basin: a geochemical approach, Appl. Geochem., 13, 593–606, 1998.

Langmuir, D.: The geochemsitry of some carbonate ground waters in central Pennsylvania, Geochim. Cosmochim. Ac., 35, 1023–1045, 1971.

Li, X. D., Harue, M., Kusakabe, M., Yanagisawa, F., and Zeng, H. A.: Degradation of groundwater quality due to anthropogenic sulfur and nitrogen contamination in the Sichuan Basin, China, Geochem. J. 40, 309–332, 2006.

López-Chicano, M., Bouamama, M., Vallejos, A., and Pulido-Bosch, A.: Factors which determine the hydrogeochemical behavior of karst springs. A case study from the Betic Cordilleras, Spain, Appl. Geochem., 16, 1179–1192, 2001.

Lü G., Zhao, L. B., Sun, X. Z., and Tan, D. F.: Periodic Summary Report on Investigating the Environmental Hydrogeology in Dalian Area, The Second Institute of Hydrogeology and Engineering Geology, Liaoning Bureau of Geology, Dalian, China, 48–66, 1981 (in Chinese).

Moral, F., Cruz-Sanjulian, J. J., and Olias, M.: Geochemical evolution of groundwater in the carbonate aquifers of Sierra de Segura (Betic Cordillera, southern Spain), J. Hydrol., 360, 281–296, 2008.

Otero, N., Canals, A., and Soler, A.: Using dual-isotope data to trace the origin and processes of dissolved sulphate: a case study in Calders stream (Llobregat basin, Spain), Aquat. Geochem., 13, 109–126, 2007.

Parkhurst, D. L. and Appelo, C. A. J.: User's guide to PHREEQC-A. computer program for speciation, reaction-path, 1-D-transport, and inverse geochemical calculation, US Geol. Surv. Water-Resour. Invest. Rep., US Geol. Surv., Denver, Colorado, 99–4259, 1999.

Plummer, L. N. and Sprinkle, C. L.: Radiocarbon dating of dissolved inorganic carbon in groundwater from confined parts of the Upper Floridan Aquifer, Florida, USA, Hydrogeol. J., 9, 127–150, 2001.

Plummer, L. N., Busby, J. F., Lee, R. W., and Hanshaw, B. B.: Geochemical modeling in the Madison aquifer in parts of Montana, Wyoming and South Dakota, Water Resour. Res., 26, 1981–2014, 1990.

Rees, C. E.: The sulphur isotopic composition of ocean water sulphate, Geochim. Cosmochim. Ac., 42, 377–381, 1978.

Sánchez-Martos, F., Pulido-Bosch, A., Molina-Sánchez L., and Vallejos-Izquierdo, A.: Identification of the origin of salinization in groundwater using minor ions (Lower Andarax, Southeast Spain), Sci. Total Environ., 297, 43–58, 2002.

Schiavo, M. A., Hauser, S., and Povinec, P. P.: Stable isotopes of water as a tool to study groundwater–seawater interactions in coastal south-eastern Sicily, J. Hydrol., 364, 40–69, 2009.

Shi, Z. S., Chen, K. Y., Shi, J., He, H. J., and Liu, B. J.: Sulfur isotopic composition and its geological significance of the Paleogene sulfate rock deposited in Dongpu Depression, Petrol. Explor. Develop., 31, 44–46, 2004 (in Chinese).

Song, Q. C.: Status quo of seawater intrusion in Daweijia karst water source of Dalian, China, Journal of Chengdu University of Technology (Science and Technology Edition), 40, 348–352, 2013 (in Chinese with English abstract).

Stuyfzand, P. J.: A new hydrochemical classification of water types with examples of application to the Netherlands, H_2O, 19, 562–568, 1986 (in Dutch).

Stuyfzand, P. J.: Base exchange indices as indicators of salinization or freshening of (coastal) aquifers, Proceedings of the, 20th Salt Water Intrusion Meeting, Naples, FL, 23–27 June 2008; Program and Proceedings book, 262–265, 2008.

Szynkiewicz, A., Witcher, J. C., Modelska, M., Borrok, D. M., and Pratt, L. M.: Anthropogenic sulfate loads in the Rio Grande, New Mexico (USA), Chem. Geol. 283, 194–209, 2011.

Szynkiewicz, A., Newton, B. T., Timmons, S. S., and Borrok, D. M.: The sources and budget for dissolved sulfate in a fractured carbonate aquifer, southern Sacramento Mountains, New Mexico, USA, Appl. Geochem., 27, 1451–1462, 2012.

Unland, N. P., Taylor, H. L., Bolton, B. R., and Cartwright, I.: Assessing the hydrogeochemical impact and distribution of acid sulphate soils, Heart Morass, West Gippsland, Victoria, Appl. Geochem., 27, 2001–2009, 2012.

Vitòria L., Otero, N., Soler, A., and Canals À.: Fertilizer characterization: isotopic Data (N, S, O, C, and Sr), Environ. Sci. Technol., 38, 3254–3262, 2004.

Vogel, J. C.: Variability of carbon isotope fractionation during photosynthesis, in: Stable Isotopes and Plant Carbon – Water Relations, edited by: Ehleringer, J. R., Hall, A. E., and Farquhar, G. D., Academic Press, San Diego, CA, 29–38, 1993.

Wang, Y. X., Guo, Q. H., Su, C. L., and Ma, T.: Strontium isotope characterization and major ion geochemistry of karst water flow, Shentou, northern China, J. Hydrol., 328, 592–603, 2006.

Wu, Q.: Study on the management model of karst groundwater system in Daweijia, Dalian City, Site Investigation Science and Technology, 1, 23–27, 1990 (in Chinese with English abstract).

Wu, Q. and Jin, Y. J.: Characteristics of seawater intrusion in coastal karst groundwater system of Daweijia area, Dalian City, Geotechnical Investigation and Surveying, 3, 43–44, 1990 (in Chinese with English abstract).

Wu, Q., Jin, Y. J., Li, D. A., and Xia, Y. H.: The mechanisms of seawater intrusion of karst groundwater system in Daweijia, Dalian City and the countermeasures of its control, The Chinese Journal of Geological Hazard and Control, 1, 64–68, 1994 (in Chinese with English abstract).

Yang, J. L.: Hydrogeochemical reactions in seawater intrusion process in Daweijia water source area, Dalian City, M.S. thesis, Jilin University (Changchun, China), 14–15, 2011 (in Chinese with English abstract).

Zhang, X. Y., Jiang, H., Zhang, Q. X., and Zhang, X.: Chemical characteristics of rainwater in northeast China, a case study of Dalian, Atmos. Res., 116, 151–160, 2012.

Zhao, C. R., Yang, J. L., Xiao, G. Q., Du, D., Pan, T., and Zhang, S. F.: Hydrogeochemical reactions and hydrogeological model for seawater intrusion processes in the Daweijia water source area, Dalian City, Geological Survey and Research, 35, 154–160, 2012 (in Chinese with English abstract).

Zhao, T. S.: Problems of karst groundwater development in littoral area and its ultimate control method, The Chinese Journal of Geological Hazard and Control, 4, 73–77, 1991 (in Chinese with English abstract).

Table 1. Hydrochemical and isotopic data of the June 2006(*) and August 2010 field sampling.

Sample	Well Depth (m)	Screened Intervals (m)	EC (µs cm^{-1})	pH	T (°C)	ORP (mV)	DO (mg L^{-1})	Ca^{2+} (mg L^{-1})	Na^{+} (mg L^{-1})	K^{+} (mg L^{-1})
Groundwater samples collected from the carbonate aquifer:										
CG4	100	70–95	1015	7.2	16.1	193	3.6	119.6	50.5	1.2
CG16	88	58–84	715	7.5	22.4	2	5.7	100.9	26.1	4.7
CG3	110	72–98	986	7.3	19.3	201	4.0	115.8	47.2	1.5
CG6	120	75–112	796	7.3	21.7	139	3.7	99.4	38.2	1.2
CG14	128	85–118	749	7.6	22.0	34	7.2	94.5	24.5	1.0
CG9	100	68–92	846	7.6	18.8	2	8.6	113.6	44.4	6.5
CG2	120	72–107	2050	6.5	16.0	186	7.5	187.7	106.0	2.3
CG7	92	59–88	1761	6.6	17.0	222	6.6	198.5	97.8	1.0
CG17	110	68–97	1370	7.0	14.2	200	7.0	149.1	82.9	1.5
CG1	100	71–93	2280	7.2	18.2	163	5.6	212.5	184.0	3.5
CG8	95	65–92	1416	7.4	20.0	199	6.1	190.6	66.7	1.4
CG11	100	67–93	2050	7.1	15.1	2	7.6	302.8	84.3	1.7
CG12	100	68–93	1362	7.3	20.0	25	7.4	183.0	81.3	1.6
CG19	62	43–59	1481	6.7	14.5	26	4.7	220.0	70.6	2.0
CG10	90	59–86	1586	7.4	21.5	214	7.4	207.7	62.0	26.4
CG1*	100	71–93	2890	7.3	14.9			284.5	312.2	3.7
CG2*	120	72–107	2110	7.0	13.2			151.2	103.2	1.5
CG3*	110	72–98	2300	7.2	13.2			158.9	175.6	3.5
Groundwater samples collected from the Quaternary aquifer:										
QG7	28	15–24	1242	7.6	13.1	2	6.7	156.2	82.1	1.0
QG3	8.4	6–7.5	821	7.0	18.3	52	4.4	118.3	28.6	4.0
QG4	14	7–13	912	7.5	23.0	22	3.6	99.1	42.5	13.1
QG5	12	7–11	1903	7.0	17.1	219	3.6	208.4	146.0	0.5
QG10	10	6–9	2210	7.2	13.9	204	5.0	128.2	286.1	12.8
QG8	15	9–14	1633	7.4	16.4	16	7.8	154.6	134.5	2.7
QG9	20	12–17	1289	7.3	20.7	23	4.4	151.4	67.8	7.6
QG11	17	8–15	2780	7.4	23.2	65	1.3	205.8	295.5	11.1
QG12	17	12–16	2210	7.0	14.2	41	5.6	274.7	154.6	2.3
QG2*	22	15–21	2310	7.0	15.2			244.9	198.5	3.6
QG11*	17	8–15	2820	7.2	13.9			153.8	229.2	4.4
SW1	Seawater sample		43 800	7.7	26.8	171	5.0	324.5	7626.0	289.1

Table 1. Continued.

Sample	Mg^{2+} (mg L^{-1})	Cl^- (mg L^{-1})	SO_4^{2-} (mg L^{-1})	NO_3^- (mg L^{-1})	HCO_3^- (mg L^{-1})	SI_{cal}	SI_{dol}	SI_{gyp}	$\delta^{34}S_{SO_4}$ (‰)	$\delta^{13}C_{DIC}$ (‰)
Groundwater samples collected from the carbonate aquifer:										
CG4	38.5	261.0	109.7	60.9	247.1	0.1	−0.07	−1.47	10.4	−9.3
CG16	16.1	112.1	82.4	77.2	101.2	0.1	−0.24	−1.58		
CG3	37.8	209.5	93.8	60.3	282.8	0.27	0.33	−1.55	10.9	
CG6	24.1	141.6	67.1	43.1	250.1	0.23	0.18	−1.41	9.0	−9.9
CG14	31.9	105.7	65.1	69.1	238.1	0.48	0.84	−1.75	6.6	−8.4
CG9	17.4	203.8	101.8	147.9	134.0	0.21	−0.14	−1.47		
CG2	48.5	288.4	189.2	263.9	199.4	−0.59	−1.53	−1.12	8.8	−9.7
CG7	51.1	892.9	240.5	334.7	145.9	−0.65	−1.65	−1.05	8.7	−12.0
CG17	38.3	343.4	134.1	278.8	163.7	−0.31	−1.01	−1.31	10.4	−9.3
CG1	72.3	561.0	201.4	282.6	282.8	0.27	0.32	−1.12	13.1	−10.6
CG8	32.1	344.5	104.1	256.6	190.5	0.38	0.27	−1.35		
CG11	42.3	937.3	249.9	579.4	205.4	0.14	−0.36	−0.9		
CG12	31.9	380.8	146.2	90.1	318.5	0.51	0.55	−1.24		
CG19	72.1	390.0	219.1	265.6	446.5	0	−0.28	−1.05		
CG10	42.4	923.5	306.9	295.7	205.4	0.35	0.31	−0.95	10.1	−11.6
CG1*	114.0	596.6	135.3	124.8	253.8	0.34	0.5	−1.23	14.0	
CG2*	48.4	323.3	142.7	321.5	174.2	−0.33	−0.97	−1.29	10.4	
CG3*	54.2	511.2	109.4	79.6	120.8	−0.28	−0.85	−1.41	14.2	
Groundwater samples collected from the Quaternary aquifer:										
QG7	27.5	254.5	54.4	146.6	262.0	0.56	0.55	−1.65	8.1	−9.4
QG3	21.6	103.3	135.4	74.7	190.5	−0.24	−0.95	−1.34	5.4	−12.8
QG4	40.0	203.3	145.2	80.2	241.1	0.34	0.6	−1.43	5.7	−14.5
QG5	44.7	281.3	254.3	337.3	199.4	−0.03	−0.48	−0.98	9.0	−11.0
QG10	51.0	640.6	211.5	156.1	309.6	0.04	−0.13	−1.27	10.1	−10.6
QG8	47.5	269.8	285.9	256.9	220.3	0.31	0.33	−1.03	7.2	−8.6
QG9	49.1	299.4	216.2	133.5	241.1	0.27	0.34	−1.15	8.6	−10.2
QG11	74.8	469.4	344.9	259.5	291.7	0.59	1.07	−0.95	9.4	−5.9
QG12	49.6	386.2	368.8	347.9	300.7	0.19	−0.16	−0.76		
QG2*	66.3	315.7	134.2	386.3	512.7	0.32	0.29	−1.23	9.5	
QG11*	69.2	448.3	207.6	190.6	200.9	−0.1	−0.35	−1.19	7.8	
SW1	978.8	16 683.9	4116.0	1092.0	163.7				20.8	−3.3

Table 2. Summary of main hydrochemical processes occurring in the carbonate and quaternary aquifer, along with evidence used to assess the process.

Aquifer (Carb/Quat)	Process	Occurring (Y/N)?	Evidence (1)	Evidence (2)	Figure
Carbonate Aquifer	Calcite dissolution (congruent)	No	Most groundwater samples with $SI_{calcite} < 0.1$ and $Ca : HCO_3 > 1 : 2$	No correlation between Ca or HCO_3 and $\delta^{13}C$	Figs. 6a and 7
	Incongruent dolomite weathering	Yes	Increase in Mg/Ca along the flow path	Increase in $\delta^{13}C$ with increasing Mg/Ca	Fig. 7a
	Cation exchange	Yes	Most samples with negative ΔNa^+ values and positive $\Delta Ca^{2+} + \Delta Mg^{2+}$ values	MixCa-Cl facies in HFE diagram	Figs. 2 and 5
	Fertilizer addition	Yes	Positive correlation between NO_3^- and SO_4^{2-} concentrations	Mass balance results from different sources of $\delta^{34}S_{SO_4}$	Figs. 8 and 10
	Gypsum dissolution	Yes	All water samples with $SI_{gypsum} < -0.5$	Ca/SO_4 ratios > 1	Fig. 6
Quaternary Aquifer	Calcite dissolution (congruent)	Minor	Lack of correlation between $\delta^{13}C$ and HCO_3; Increasing $\delta^{13}C$ with increasing Ca	Most groundwater samples with $SI_{calcite} < 0.1$ and $Ca : HCO_3$ around 1 : 2	Figs. 6a and 7
	Incongruent dolomite weathering	No (apart from QG3)	$SI_{dolomite} > -0.5$; $Mg : HCO_3 > 1 : 4$	No obvious increasing trend in $\delta^{13}C$ with increasing Mg/Ca	Figs. 6b and 7
	Cation exchange	Yes	Enrichment in Ca and loss of Na along flow path	$SI_{calcite}$ and $SI_{dolomite}$ close to or exceeding 0	Fig. 2
	Addition of sulphate from fertilizer	Yes	Positive relationship between SO_4 and NO_3	Increasing $\delta^{34}S$ values with increasing NO_3 concentrations	Figs. 8 and 10
	Gypsum dissolution	Yes	$Ca : SO_4$ close to 1	$SI_{gyp} < -0.5$	Fig. 6c

Title Page
Abstract Introduction
Conclusions References
Tables Figures
◀| |▶
◀ ▶
Back Close
Full Screen / Esc
Printer-friendly Version
Interactive Discussion

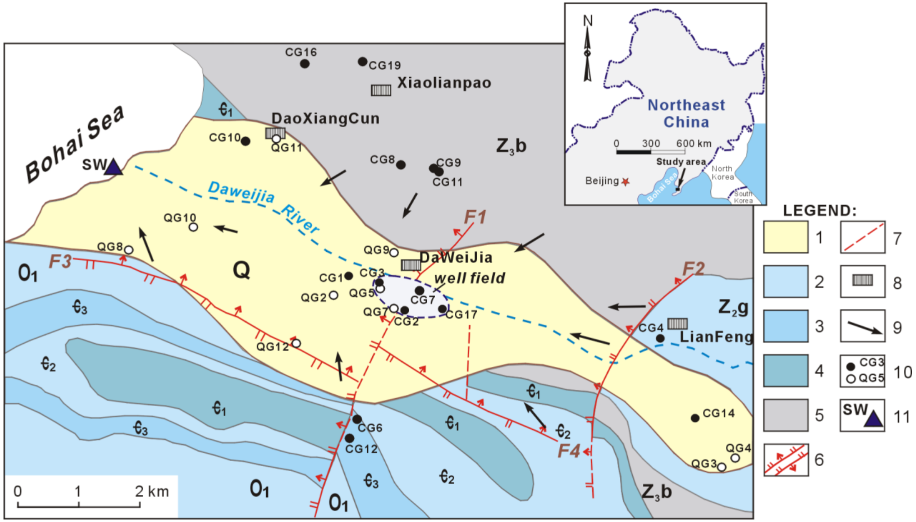

Figure 1. Geological setting and water sampling locations. Geology modified after Wu and Jin (1990). Formation note: O1 – Lower Ordovician; F_3 – Upper Cambrian; F_2 – Middle Cambrian; F_1 – Lower Cambrian; Z_2g – Ganjingzi group of Middle Sinian; Z_3b – Beishan group of Upper Sinian. Legend: 1 – Quaternary sediments; 2 – thick-beded limestone; 3 – laminated limestone with shale; 4 – argillaceous limestone; 5 – sandstone and shale; 6 – normal/thrust fault; 7 – buried fault; 8 – town location; 9 – approximate groundwater flow direction; 10 – sampling wells • from deep carbonate aquifers (depth > 80 m), ∘ from shallow Quaternary aquifer (depth < 40 m); 11 – sampling site for seawater.

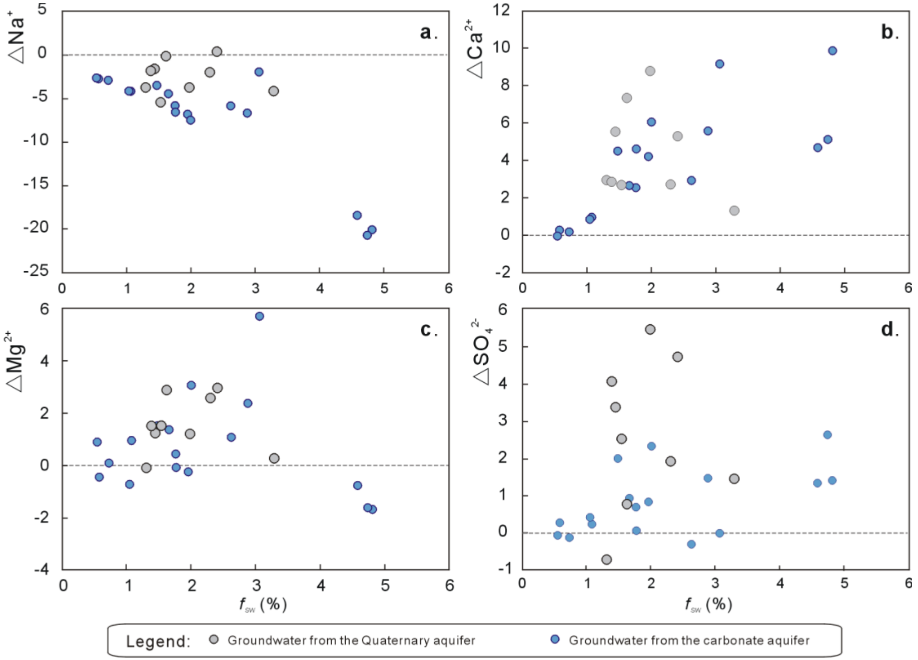

Figure 2. Graphs showing the cationic Δ-values of groundwater samples vs. fraction of seawater: **(a)** ΔNa^+; **(b)** ΔCa^{2+}, **(c)** ΔMg^{2+}, and **(d)** ΔSO_4^{2-}.

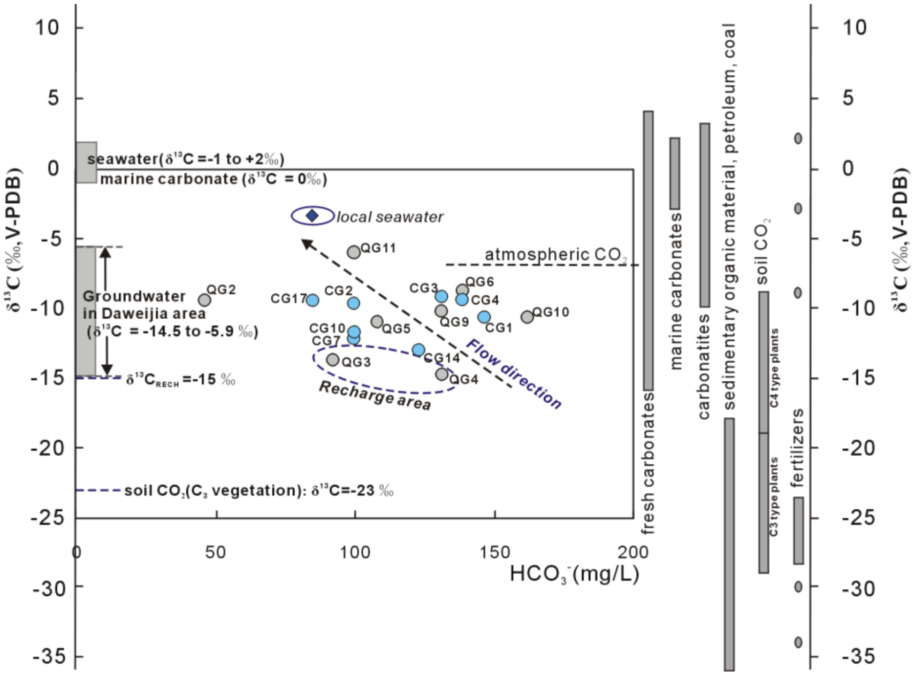

Figure 3. $\delta^{13}C_{DIC}$ vs. dissolved inorganic carbon for the groundwater samples (August 2009) in the Daweijia area, comparing with $\delta^{13}C$ values for the main carbon reservoirs (Vitòria et al., 2004 and therein). See Fig. 2 for legend.

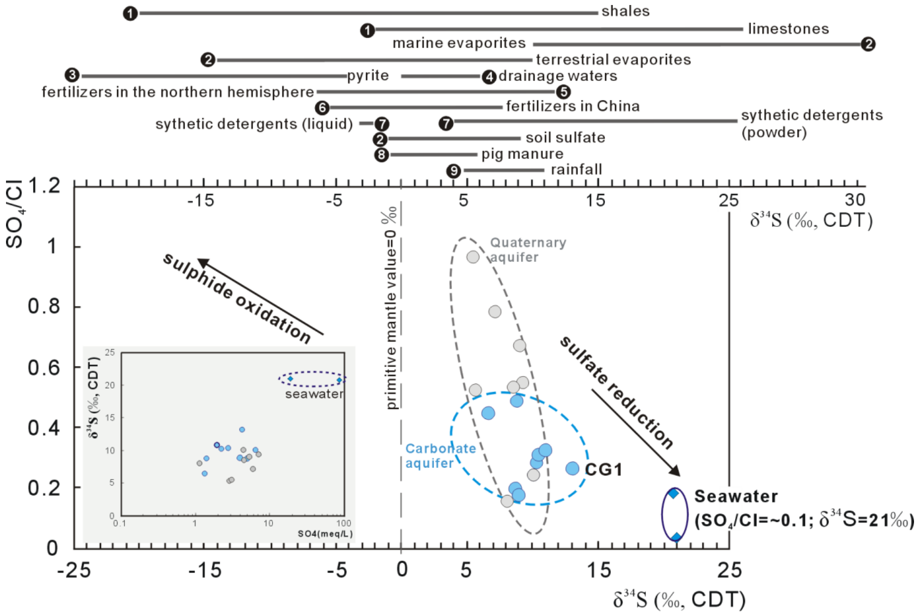

Figure 4. δ^{34}S of dissolved SO_4 vs. SO_4/Cl for groundwater samples from the Daweijia area. The range of sulfur isotopic values of some major sulfur reservoirs and selected materials is summarized from literature compiled data as follows: 1 – Clark and Fritz (1997); 2 – Vitòria et al. (2004); 3 – Szynkiewicz et al. (2012); 4 – Unland et al. (2012); 5 – Szynkiewicz et al. (2011); 6 – Li et al. (2006); 7 – Hosono et al. (2007); 8 – Cravotta (1997) and Otero et al. (2007); 9 – Hong et al. (1994). See Fig. 2 for legend.

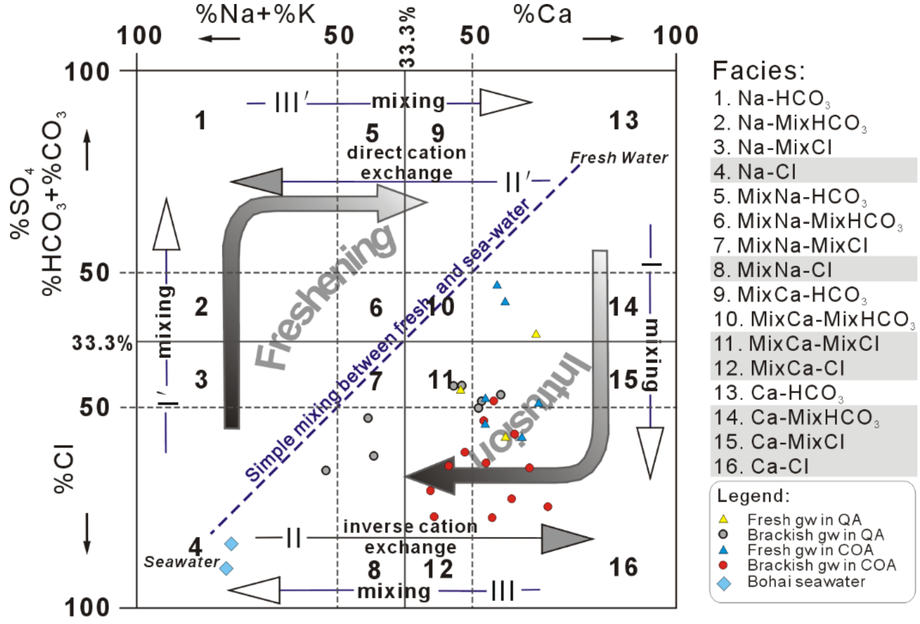

Figure 5. Hydrogeochemical Facies Evolution (HFE) diagram.

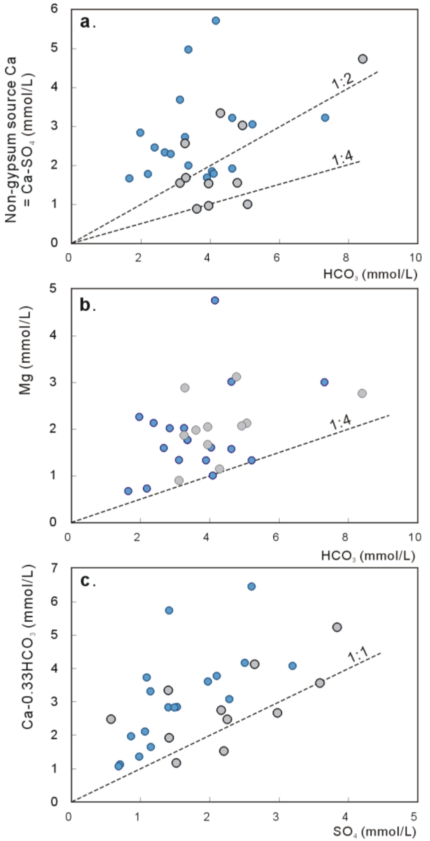

Figure 6. Graphs showing **(a)** non-gypsum source Ca^{2+} vs. HCO_3^-; **(b)** Mg^{2+} vs. HCO_3^- concentrations for groundwater samples in Daweijia area. In **(a)**, the 1 : 2 and 1 : 4 relationship lines suggest congruent dissolution of calcite and dolomite, respectively. In **(b)**, the 1 : 4 relationship line suggests congruent dissolution of dolomite. In **(c)**, the theoretical relationship of 1 : 1 indicates congruent dissolution of gypsum. See Fig. 2 for legend.

Title Page
Abstract
Introduction
Conclusions
References
Tables
Figures
◀
▶
◀
▶
Back
Close
Full Screen / Esc
Printer-friendly Version
Interactive Discussion

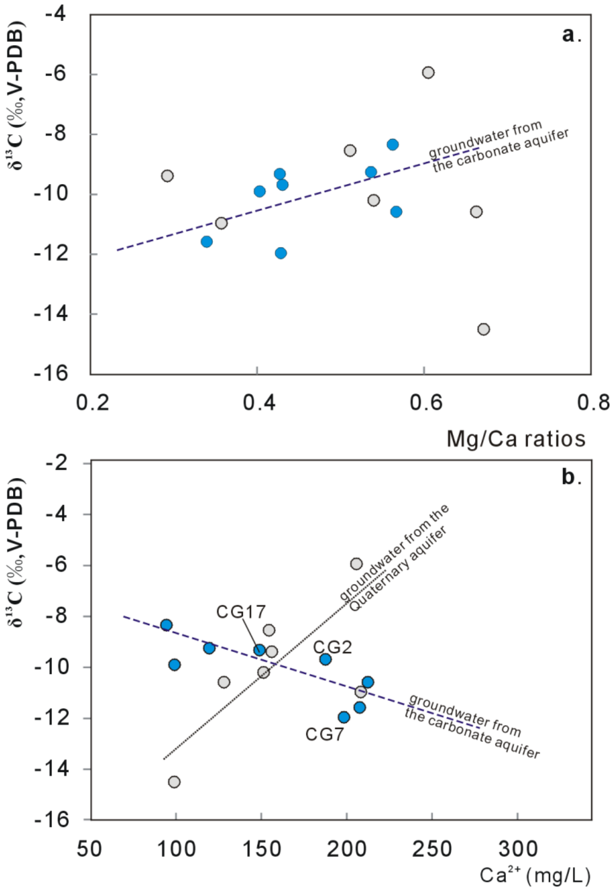

Figure 7. Graphs showing **(a)** Mg/Ca ratios (by meq L^{-1}); **(b)** Ca^{2+} concentrations vs. $\delta^{13}C_{DIC}$ values in different aquifers (grey – groundwater samples collected from the Quaternary aquifer; blue – groundwater samples collected from the carbonate aquifer).

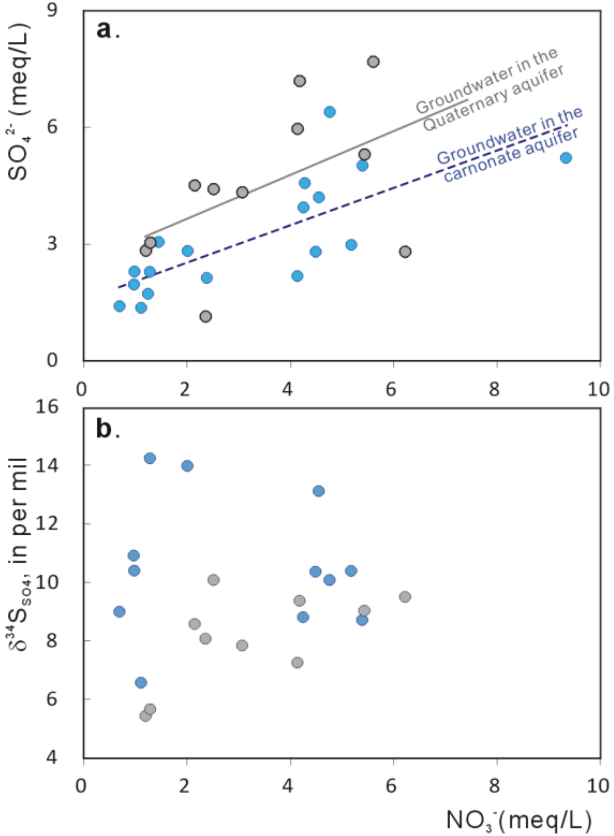

Figure 8. Bivariate plots for **(a)** relationship between SO_4^{2-} and NO_3^- concentration and **(b)** $\delta^{34}S_{SO_4}$ vs. NO_3^- concentrations. See Fig. 2 for legend.

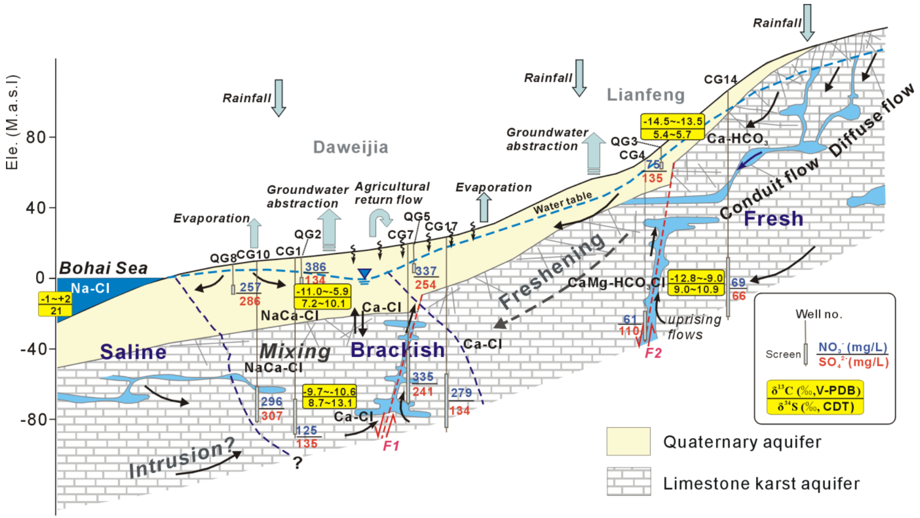

Figure 9. Conceptual model showing the hydrogeological system (modified after Yang, 2011) and NO_3^- and SO_4^{2-} concentrations and sources, with characteristic ranges of $\delta^{13}C$ and $\delta^{34}S_{SO_4}$ values (showing a vertically increasing trend). Arrows in aquifers indicate general groundwater flow direction.

HESSD
12, 11331–11370, 2015

Identification of anthropogenic and natural inputs of sulfate
D. Han et al.

Title Page
Abstract
Introduction
Conclusions
References
Tables
Figures
◀◀
▶▶
◀
▶
Back
Close
Full Screen / Esc
Printer-friendly Version
Interactive Discussion

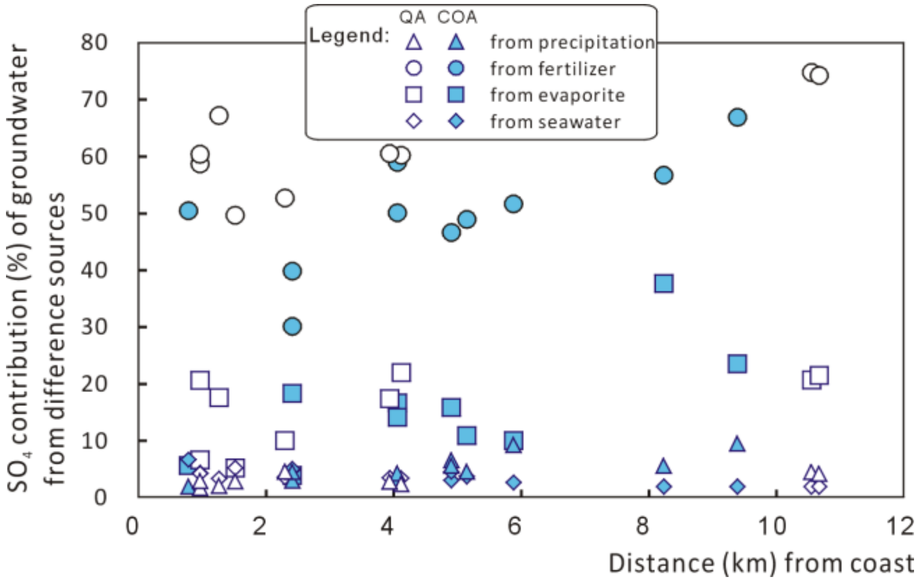

Figure 10. Calculated SO_4^{2-} contribution of groundwater from four different sources (QA – groundwater from the Quaternary aquifer; COA – groundwater from the carbonate aquifer).